HHS Public Access

Author manuscript

J Vasc Res. Author manuscript; available in PMC 2020 July 04.

Published in final edited form as:

J Vasc Res. 2019 ; 56(5): 217–229. doi:10.1159/000501312.

Effects of Iliac Stenosis on Abdominal Aortic Aneurysm Formation in Mice and Humans

Gurneet S. Sangha[a], **Albert Busch**[c], **Andrea Acuna**[a], **Alycia G. Berman**[a], **Evan H. Phillips**[a], **Matthias Trenner**[c], **Hans-Henning Eckstein**[c], **Lars Maegdefessel**[c], **Craig J. Goergen**[a,b]

[a]Purdue University, Weldon School of Biomedical Engineering, West Lafayette, IN, USA

[b]Purdue University, Purdue University Center for Cancer Research, West Lafayette, IN, USA

[c]Technical University Munich, Department for Vascular and Endovascular Surgery, Munich Aortic Center, Klinikum rechts der Isar, Munich, Germany

Abstract

Reduced lower-limb blood flow has been shown to lead to asymmetrical abdominal aortic aneurysms (AAAs) but the mechanism of action is not fully understood. Therefore, small animal ultrasound (Vevo2100, FUJIFILM VisualSonics) was used to longitudinally study mice that underwent standard porcine pancreatic elastase (PPE) infusion ($n = 5$), and PPE infusion with modified 20% iliac artery stenosis in the left ($n = 4$) and right ($n = 5$) iliac arteries. Human AAA computed tomography images were obtained from patients with normal ($n = 9$) or stenosed left ($n = 2$), right ($n = 1$), and bilateral ($n = 1$) iliac arteries. We observed rapid early growth and rightward expansion (8/9 mice) in the modified PPE groups ($p < 0.05$), leading to slightly larger and asymmetric AAAs compared to the standard PPE group. Further examination showed a significant increase in TGFβ1 ($p < 0.05$) and cellular infiltration ($p < 0.05$) in the modified PPE group versus standard PPE mice. Congruent, yet variable, observations were made in human AAA patients with reduced iliac outflow compared to those with normal iliac outflow. Our results suggest that arterial stenosis at the time of aneurysm induction leads to faster AAA growth with aneurysm asymmetry and increased vascular inflammation after 8 weeks, indicating that moderate iliac stenosis may have upstream effects on AAA progression.

Keywords

Aneurysm; Asymmetry; Iliac artery; Murine

Dr. Craig J. Goergen, Purdue University, Weldon School of Biomedical Engineering, 206 S. Martin Jischke Dr., West Lafayette, IN 47907 (USA), cgoergen@purdue.edu.

Author Contributions

All authors helped in designing the experiment, interpreting the data, and providing critical revisions to this manuscript. A.B. performed all PPE infusion and iliac ligation procedures as well as histochemical analysis. Small animal ultrasound imaging and data analysis was performed by G.S.S., A.A., A.G.B., and E.H.P. Funding for all experimental procedures was obtained by A.B., L.M., and C.J.G.

Statement of Ethics

The study was performed with approval from the Purdue Animal Care and Use Committee and according to the Guidelines of the World Medical Association Declaration of Helsinki. The Ethics Committee of Klinikum rechts der Isar, Technische Universitat Munchen approved the study, and written informed consent was given by all patients.

Disclosure Statement

The authors have no conflict of interest to declare.

Introduction

Abdominal aortic aneurysms (AAAs) are a complex and often asymptomatic disease affecting 5–10% of men between the ages of 65 and 79 years [1–3]. AAA pathophysiology is associated with destruction of elastin and increased collagen turnover in the medial and adventitial layers, resulting in dilation of the vessel. This dilation and change in material properties weakens the arterial wall, increasing the likelihood of life-threatening aortic rupture. The initiation and progression of this disease, however, is multifactorial and influenced by a combination of environmental and genetic factors. AAA growth is coupled with proteolytic degradation of aortic connective tissue, inflammation and immune responses, and increased biomechanical wall stress [4]. The multifactorial nature of aneurysm progression leads to an increased risk of aortic rupture in some patients more than in others.

One underinvestigated area of AAA research is how changes in lower-extremity flow alter infrarenal aortic hemodynamics and aneurysm expansion. Altered iliac artery flow can be caused by a myriad of factors including atherosclerotic plaque formation, above-knee amputations, or muscular inactivity. Vollmar et al. [5] first observed the phenomenon that above-knee amputees developed AAAs that expanded asymmetrically in a study of 1,031 veterans. Not only were AAA more prevalent in the amputee group (5.8 vs. 1.1%), but these patients also developed asymmetric AAAs that expand towards the amputated side of the body. The authors hypothesized that a higher incidence of asymmetric AAAs may be due to complex flow patterns in amputees near the aortic bifurcation that cause abnormal mechanical shear stress on the vessel. A later study by Lorenz et al. [6] found that among 545 surgical AAA patients, the incidence of AAA in groups with above and below the knee lower-limb amputation, compared to controls, were statistically indistinguishable after controlling for atherosclerosis risk factors. This study, however, did not investigate the longitudinal effects of altered iliac artery hemodynamics on AAA geometry. Nevertheless, exploring the factors contributing to AAA asymmetry can improve our understanding of how hemodynamics affects AAA formation. Indeed, previous AAA biomechanics studies have shown that aortic curvature and diameter asymmetry are important markers in rupture-risk assessment [7–10], most likely due to the geometric influences on wall stress [7, 11]. In fact, Crawford et al. [12] showed that altered aortic outflow is associated with AAA rupture at smaller diameters. This suggests that identifying additional metrics may help to develop patient-specific aneurysm growth and risk stratifications.

Additional small animal work has been performed to investigate the effects of altered lower-limb outflow on AAA progression. Hoshina et al. [13] showed that rats that had undergone porcine pancreatic elastase (PPE) infusion with left femoral arteriovenous fistula experienced increased aortic wall shear stress of 300% compared to reduced shear stress of 60% in animals that underwent left iliac artery ligation. A comparison of AAA diameters showed that mice that had undergone iliac artery ligation had aortic diameters that were almost twice the size of the femoral arteriovenous fistula groups. Moreover, studies using similar models have shown that reduced wall shear stress induced by iliac ligation may also affect endothelium stability and permeability [14] and medial-adventitial angiogenesis [15],

leading to transmural aortic inflammation. Together, these human and animal studies suggest that altered iliac artery hemodynamics and mechanics have upstream effects on the aorta, thereby potentially exacerbating AAA progression, influencing unilateral growth and eventual rupture rates. The presented study utilized longitudinal small animal ultrasound imaging to assess structural and hemodynamic changes in the infrarenal aorta of mice after PPE infusion in combination with modified unilateral iliac stenosis. Additionally, we assessed gene expression and histological changes between mice that had undergone the standard and modified PPE procedures. Our murine results were then compared to human AAA data with and without iliac artery stenosis. We hypothesized that *moderate iliac artery stenosis* would create regions of disturbed aortic flows, thus causing gene expression and hemodynamic changes within the infrarenal aorta that lead to asymmetric AAA formation with expansion direction correlating to the side of stenosis.

Materials and Methods

Elastase Infusion Surgery

Ten-week-old male C57BL/6J wild-type mice from The Jackson Laboratory (Bar Harbor, ME, USA) underwent PPE infusion surgeries. The Purdue Animal Care and Use Committee approved all procedures. Mice were separated into standard PPE ($n = 5$), left partial ligation PPE ($n = 4$), and right partial ligation PPE ($n = 5$) groups. All animals were anesthetized, and aseptic technique was used during the procedure. The infrarenal aorta was exposed and infused with 2 U/mL of PPE for 10 min (online suppl. Text S1; see www.karger.com/doi/10.1159/000501312 for all online suppl. material). The left or right iliac artery was partially ligated by tying a 6–0 silk-braided suture around both the iliac artery and a 30-gauge needle. The needle was then removed, resulting in vessel stenosis as described previously (online suppl. Fig. 1) [16].

Ultrasound Imaging

Mice were imaged using a high-resolution small animal ultrasound system (Vevo2100, FUJIFILM VisualSonics) with a 22–55 MHz transducer (MS550D; 40 MHz center frequency; online suppl. Fig. 2). We acquired full ultrasound imaging datasets for all mice prior to surgery (day 0) and on days 3, 7, 14, 21, 28, and 56 after surgery. Long-axis B-mode (Fig. 1a, b) was used to assess vessel diameter, and M-mode (Fig. 1c, d) was used to quantify circumferential cyclic Green-Lagrange strain. Mean and peak blood flow velocities were quantified from pulsed-wave Doppler (PWD) images (Fig. 1e, f) in the middle of the infrarenal aorta, and proximal and distal regions of the iliac arteries. Finally, 3D-gated acquisitions of the infrarenal aorta and iliac arteries was performed using a stepper motor that translated across the abdomen on the animal with a step size of 193 μm. Further details are described in online supplementary Text S2–3.

Murine and Human 3D Segmentation and Centerline Deviation Quantification

We performed 3D segmentation and centerline deviation analysis using the SimVascular platform [17] on day 0, 28, and 56 murine datasets. Day 0 segmentation was used to assess the morphology of the healthy aorta, which was then used to determine the projected healthy aorta at later time points for comparison (online suppl. Text S4). We then calculated the

AAA and healthy aortic centerline paths, by identifying the centroid of both segmentations in a short-axis view, to quantify the magnitude and direction of aneurysm expansion. The same centerline deviation protocol was applied to acquired computed tomography images from 9 “standard” AAA patients without iliac stenosis and 4 “modified” patients with either left iliac ($n = 2$), right iliac ($n = 1$), or both left and right iliac artery ($n = 1$) high-grade stenosis. The study was performed according to the Guidelines of the World Medical Association Declaration of Helsinki. The Ethics Committee of Klinikum rechts der Isar, Technische Universiät München approved the study, and written informed consent was given by all patients. Computed tomography scan images were obtained in the arterial phase and acquired by injecting 120 mL of contrast agent (Imeron®) in AAA patients in a supine position with an image acquisition time of approximately 4 min. The aortic location of maximum diameter or curvature in cases of tortuous aneurysms was used as representative centerline deviation for comparison between animals/patients.

Histology, Gene Expression, and Immunohistochemistry Experiments

The infrarenal aorta was resected en bloc with the adjacent vena cava and kidneys. The bottom half of this tissue segment was dissected to separate the aorta from adjacent tissues, stored in RNA later (Qiagen), and snap-frozen in liquid nitrogen for storage at −80 ° C. The upper half and adjacent tissues were fixed in 4% paraformaldehyde (Thermo Fisher Scientific) overnight for hematoxylin and eosin (H&E) and Elastica van Gieson (EvG) histology, as well as Ki67 and TGFβ1 immunohistochemistry. ImageJ was used to determine the cellular content in H&E sections by quantifying cell nuclei in three separate randomly chosen 50 × 50 μm^2 regions for each histological section that included the aortic intima and media at 100x magnification [18, 19]. Quantitative RT-PCR was used to assess IL-6, VEGFA, KLF4, and TGFβ1 expression in all PPE-infused mice after euthanasia on day 56. All fold changes were expressed compared to control aortae obtained from 12- to 14-week-old healthy male C57BL/6J wild-type mice ($n = 6$). Finally, Ki67 and TGFβ1 immunohistochemistry was performed overnight with primary antibody (Ki67 1:200, Abcam; TGF-b-1 1:100, Abcam) incubation at 4 ° C followed by 30 min incubation in secondary antibody (goatantirabbit,1:200 in PBS-T 5% goat serum). Further details are provided in online supplementary Text S5–7.

Human AAA Tissue Acquisition

Human aneurysm tissues were acquired from 2 AAA patients, 1 with complete occlusion of the left common iliac artery and 1 with a right above the knee amputation (online suppl. Case Report 1–2). These patients had undergone open AAA repair with patients’ informed and written consent and with approval of the local ethics committee. Samples were taken from opposite sides of the aneurysm sac and stained with H&E and EvG, as well as labeled with anti-CD34 and CD45 antibodies (Abcam) for immunohistochemistry as described previously [20].

Statistical Analysis

We used analysis of variance (ANOVA) with Tukey’s HSD post-hoc analysis to determine statistical significance for diameter, volume/length, strain, velocity, ΔCt gene expression, cell counting, and centerline deviation magnitude data. Assumptions of normality were

verified with the Shapiro-Wilk test, and any violations corrected with an inverse transformation prior to parametric statistical testing. MATLAB CircStat Toolbox was used for centerline deviation direction statistics [21]. All values are reported and plotted as average ± standard deviation, and statistical significance was determined at the $p < 0.05$ threshold. More details are provided in online supplementary Text S8.

Results

Morphological Changes in Murine Aorta before and after the PPE Infusion Procedure

We observed a rapid increase in aortic diameter (Fig. 2a, d) at day 14 for both the standard PPE (0.71 ± 0.06 mm to 1.1 ± 0.03 mm; $p < 0.001$) and modified PPE (0.71 ± 0.05 mm to 1.1 ± 0.12 mm;$p < 0.001$) groups compared to day 0. Interestingly, modified PPE diameter reached statistically significant expansion by day 3 ($p < 0.001$) compared to day 7 for the standard PPE group ($p < 0.01$). The aortic diameter then steadily increased to 1.2 ± 0.04 mm for the standard PPE group and 1.3 ± 0.15 mm for the modified PPE group by day 56 ($p = 0.89$). Aortic volume/length (Fig. 2b, e, g) followed a similar trend with the modified PPE group experiencing rapid expansion in the first 7 days (0.48 ± 0.07 mm^3/mm to 0.67 ± 0.06 mm^3/mm; $p < 0.001$) and comparatively slower growth in the standard PPE group until day 14 (0.40 ± 0.09 mm^3/mm to 0.51 ± 0.04 mm^3/mm; $p < 0.05$). At day 7, the modified PPE volume/length was statistically greater than the standard PPE group ($p < 0.05$). After this rapid expansion period, the volume/length steadily increased to 0.69 ± 0.14 mm^3/mm for the standard PPE group and 0.76 ± 0.14 mm^3/mm for the modified PPE group ($p = 0.95$; online suppl. Fig. 3). Conversely, our results showed an overall decrease in infrarenal aorta mean velocity and a significant decrease in average peak velocity between days 0 and 56 for all PPE-treated animals. Moreover, we observed an abrupt decrease in Green-Lagrange circumferential cyclic strain measurements (Fig. 2c, f) in the first 7 days after the procedure, with an overall decrease from 11.7 ± 2.6% to 3.1 ± 0.61% ($p < 0.01$) for the standard PPE group and 12.2 ± 3.6% to 3.63 ± 0.91% ($p < 0.01$) for the modified PPE group. Circumferential cyclic strain remained stable for both the proximal and distal regions of the PPE-infused aorta. Velocity and circumferential cyclic strain were higher in the modified PPE group compared to standard PPE, but this difference was not statistically significant. Individual animal ultrasound measurements can be found in online supplementary Figure 4.

In the iliac arteries, we also quantitatively assessed the effect of vessel stenosis on changes in arterial structure and hemodynamics (Fig. 3a, b). Day 56 diameter measurements distal to suture placement showed that the partially ligated iliac artery diameter (0.50 ± 0.07 mm) was significantly smaller compared to both standard (0.62 ± 0.063 mm; $p < 0.001$) and modified contralateral control (0.59 ± 0.10 mm;$p < 0.001$) iliac artery diameters. Further analysis showed iliac artery stenosis of 21% in the right iliac artery PPE group and 19% in the left iliac artery PPE group. Conversely, we did not see significant changes in vessel diameter proximal to sutures with values of 0.67 ± 0.07 mm in the standard PPE group, 0.67 ± 0.09 mm in the modified contralateral control arteries, and 0.69 ± 0.06 mm in the partially ligated arteries (Fig. 3c). Interestingly, substantial changes were not observed in iliac artery mean velocity among standard, contralateral control, and partially ligated arteries at day 56. In fact, the standard PPE group showed larger and highly variable meanvelocity

measurements compared to the modified and contralateral control iliac arteries (Fig. 3d; online suppl. Table 1). Mean and peak velocity data can be found in online supplementary Figure 4. Finally, assessment of day 56 vessel pulsatility distal to suture placement (Fig. 3e) showed that the modified iliac arteries had significantly decreased circumferential cyclic strain (2.31 ± 1.13%) compared to the contralateral control vessels (14.2 ± 4.09%; $p < 0.001$) and unmodified iliac arteries in the standard PPE group (11.9 ± 2.48%; $p < 0.001$). Together, these results indicate that the modified iliac arteries have decreased luminal diameter and patency distal to suture placement.

Aortic segmentation and centerline deviation analysis (Fig. 4a) was performed on short-axis B-mode images (Fig. 4b) to assess the magnitude (Fig. 4c) and direction (Fig. 4d) of aneurysmal shift in left and right partial iliac ligation groups compared to the standard PPE groups. Day 28 and 56 data analysis showed that standard PPE aortae expansion was heterogeneous, with the mean centerline deviation close to the origin of the Cartesian plane. Interestingly, the left and right partial iliac ligation PPE groups deviated further from the center, suggestive of more asymmetric expansion (Fig. 4e). Specifically, day 28 results suggest that the left partial iliac ligation PPE group had a centerline shift towards the rightward direction,while the right partial iliac ligation PPE group had a centerline shift towards the leftward direction (online suppl. Table 2). This trend shifts by day 56 where we observed rightward expansion in 8 out of 9 modified PPE animals (online suppl. Table 2).

Murine Histology, Gene Expression, and Immunohistochemistry Results

Based on the H&E-stained sections, we observed that standard and modified PPE mice experienced aortic wall thickening (online suppl. Fig. 5) with elastin degradation, collagen turnover, and inflammation not observed in control aortae. Magnified EvG images further confirm varying elastin degradation throughout the aorta in both the standard (Fig. 5a, b) and modified (Fig. 5c, d) groups. Moreover, we observed relatively consistent aortic wall thickness on both the left and right sides of the modified aortae suggesting homogeneous collagen deposition in the diseased vessels. Qualitative Ki67 immunohistochemistry analysis revealed increased cell proliferation in PPE-infused animals (Fig. 5f) with greater signaling in the modified PPE (online suppl. Fig. 5E) compared to the standard PPE (online suppl. Fig. 5D) aortae. An in-depth examination of nuclei showed a statistically significant increase in cell number for the standard ($p < 0.01$) and modified ($p < 0.001$) PPE groups compared to untreated controls, as well as between standard and modified PPE groups ($p < 0.05$; Fig. 5e).

For further validation, we measured upregulation of growth factor and inflammatory genes. In the standard group, the inflammatory cytokine IL-6 (5.1 ± 3.8 fold increase; Fig. 6a) and AAA-associated growth factors VEGFA (1.7 ± 0.20 fold increase; Fig. 6b) and TGF(3l (3.0 ± 1.8 fold increase; $p < 0.05$; Fig. 6c) were all upregulated compared to control aortae. The flow-dependent transcription factor KLF4 was downregulated (0.66 ± 0.24 fold change; Fig. 6d). These results are also consistent with our modified group where we observed upregulation of IL-6 (3.6 ± 1.4 fold increase), VEGFA (3.0 ± 1.9 fold increase), and TGF(3l (6.6 ± 1.9 fold increase; $p <0.0001$). On the protein level, immunohistochemistry confirmed higher expression of TGFpi in standard (online suppl. Fig. 5G, J) and modified PPE (online suppl. Fig. 5H, K) when compared to control aortae (online suppl. Fig. 5I, L). Interestingly,

we observed statistically significant increases in TGFβ1 between the standard and modified groups ($p < 0.05$). Modified KLF4 expression showed large variation from the mean with downregulation in the left PPE group (0.69 ± 0.24 fold decrease) and upregulation in the right PPE group (1.6 ± 1.2 fold increase).

Human AAA Centerline, Histology, and Immunohistochemistry Results

Aortic segmentation and centerline deviation analysis (Fig. 7a, b) was performed on human AAA data to assess the magnitude and direction of aneurysm growth (Fig. 7c). Overall, we observed that the healthy iliac (standard) AAA group had an average centerline deviation of 13.8 ± 13.35 mm and the iliac stenosis/occlusion (modified) group had an average centerline deviation of 12.9 ± 4.43 mm ($p = 0.33$). Interestingly, we saw anterior and leftward expansion of the AAA away from the spine and inferior vena cava for both the standard (75.5 ± 25.6°) and modified (46.0 ± 13.8°) groups (Fig. 7d). A closer look at the human datasets show that the center of the standard healthy aorta was shifted leftward laterally with respect to the center of the spine with a distance of 5.72 ± 3.08 mm. Patients with left or right iliac occlusion had an increased leftward lateral shift of 10.6 ± 1.93 mm, while the patient with both iliac occlusions had a leftward lateral shift of 2.05 mm. Finally, histological analysis was performed on the left and right lateral sides of the aneurysm sac, at the level of maximum diameter, for 2 patients with either left iliac artery occlusion or right-knee amputation. Different lateral aneurysm wall morphology and cellular content was seen with H&E and EvG staining, as well as CD34 and CD45 immunohistochemistry (online suppl. Fig. 6). Examination of H&E staining of the left side of the AAA sac showed increased cellular infiltration, while EvG staining revealed extensive breakdown of elastin laminar units throughout the AAA. CD34 and CD45 staining revealed increased inflammatory infiltration on the left side of the aneurysm for both AAA patients. Overall, we observed distinct difference in histomorphology when comparing the left and right side of these aneurysms, as well as inflammatory activity (CD45) and angiogenesis (CD34).

Discussion

In this study, we investigated the effects iliac stenosis has on asymmetric AAA formation. This work was motivated by the observation that patients with above the knee amputations formed asymmetrical AAAs, potentially due to disturbed flows that produce high shear zones and increased mechanical stress on the aortic wall [5]. Therefore, we attempted to replicate this phenomenon in asmall animal model of AAAs to study how vessel hemodynamics longitudinally affects AAA formation and growth. Understanding asymmetrical AAA formation is important, as disturbed iliac flow may lead to increased endothelium permeability and medial-adventitial angiogenesis, both of which have been shown to increase aortic inflammation that can potentially exacerbate AAA development and rupture [14, 15, 22].

The PPE infusion murine model combined with an iliac artery stenosis was used to evaluate the effects restricted lower-limb blood flow has on aneurysm formation in the infrarenal aorta as previously presented by Vollmar et al. [5]. Low-dose PPE (2 U/mL) was utilized to create aneurysms that mimic early AAA progression, and male mice were used in this initial

study as AAA disproportionally affects men and to minimize sex-specific effects. Our gene expression results confirmed that low-dose PPE induces an inflammatory response as shown by the upregulation of IL-6 [23, 24] and VEGFA [25] in both the standard and modified PPE groups, suggesting upregulation of extracellular matrix proteinases [23]. Histological analysis of standard and modified PPE groups showed diffuse elastin breakdown with the modified PPE group having greater cell infiltration compared to the standard PPE group ($p < 0.05$). Additionally, ultrasound imaging showed a reduction in arterial velocity and a 61% increase in volume/length from days 0 to 56, as well as a rapid reduction in circumferential cyclic strain, providing quantitative evidence of decreased pulsatility due to changes in arterial material properties. These results are consistent with previous works that show that a low concentration of PPE results in elastin degradation and collagen turnover, both of which result in hemodynamic and morphological changes in the vessel [16, 26]. Lastly, a decrease in iliac circumferential cyclic strain distal to the suture placement provided evidence that the partial iliac artery ligation increased peripheral vessel stiffness.

AAA asymmetry was quantified by performing 3D segmentation of the projected healthy, standard PPE, and modified PPE infrarenal aortae, followed by the quantification of the magnitude and direction of centerline deviation. Previous work has shown PPE-induced dynamic changes in centerline deviation up to day 28 after PPE infusion in mice [27]; therefore, we increased the length of our study to 56 days to quantify the effects of iliac stenosis on centerline deviation over a longer timeframe. Interestingly, day 56 results showed that both the left and right PPE groups had a rightward centerline shift (8 of 9 mice), possibly due to supportive surrounding tissues and a new equilibrium of proteolytic and stabilizing aortic wall activity. Assessment of the iliac artery PWD showed only antegrade blood flow, suggesting that iliac stenosis alone may not be enough to induce disturbed retrograde flows in the infrarenal aorta. In fact, mice do not experience reversal of flow in the infrarenal aorta as commonly observed in healthy humans, thus highlighting species-specific hemodynamic differences that may account for the lack of exacerbated aortic disturbed flow [28].

Pulsed wave velocity, however, provides bulk flow information along the beam axis and lacks the capability to detect small changes in velocities along the vessel wall that may induce abnormal shear stress [29]. Therefore, we assessed changes in endothelial flow-dependent KLF4 gene expression [30] which showed a limited trend between the standard and modified PPE groups. Specifically, we saw KLF4 downregulation in the left iliac stenosis PPE group and upregulation in the right iliac stenosis group, thus creating large variability the combined modified group. We did, however, observe a significant decrease in the modified left iliac artery mean and peak velocities at days 28 ($p < 0.001$) and 56 ($p < 0.05$). Additional quantification of iliac artery structure and hemodynamics showed similar proximal diameter and velocity values between the modified iliac artery and contralateral control. Characterization of distal iliac artery showed variable changes in blood flow velocity but did show significant decrease in circumferential cyclic strain and approximately 20% stenosis compared to the day 0 baseline measurements. These results suggest modest changes in iliac artery mechanics that may have had upstream effects on the aorta, which accelerated early murine aneurysm growth. One possible explanation for the lack of significant flow changes in the iliac arteries is the moderate stenosis of the iliac artery

combined with the possible formation of collateral vessels over the 8-week period in response to decreased blood flow to the lower limb [31]. Another consideration is that murine aortae trifurcate into the left and right iliac artery, as well as a tail artery. Significant flow changes in the iliac arteries may also be mitigated due to compensations caused by tail artery remodeling. Interestingly, we observed a significant upregulation of TGFp1 in the modified PPE groups relative to the standard group ($p < 0.05$). While the role of TGFp1 on AAA progression is still somewhat uncertain [32,33], silencing has been shown to prevent AAA formation in PPE infusion and angiotensin II murine models [32, 34]. This suggests that the upregulation of TGFp1 reported here may be promoting AAA formation in animals with partial iliac ligation. Closer examination of the data also revealed that mice with modified iliac outflow experience rapid early aneurysm growth in the first 7 days after AAA induction compared to mice without iliac stenosis ($p < 0.05$). This is interesting as the time between aneurysm induction and growth plateau is considered the most active arterial remodeling period in the murine PPE infusion model [35]. Future work could utilize other mouse models, such as the topical periadventitial PPE applications [36,37], where significant arterial remodeling can be observed beyond 3 weeks of AAA induction due to pronounced inflammatory activity [39]. Additionally, sample size should also be increased by additional studies to improve the power of the results and to more clearly resolve gene expression differences between groups. Taken together, while retrograde flow was not detected with our methods, there could be fine changes in the iliac artery mechanics and hemodynamics that have upstream implications in AAA induction and growth.

Finally, centerline deviation was also quantified in human AAAs to better elucidate the effects of iliac atherosclerotic disease and AAA development. Quantifying computed tomography data from 13 AAA patients (9 controls and 4 with high-grade iliac stenosis) revealed that on average, aneurysms shifted both in the anterior and leftward directions. While the number of patients is small, this expansion could be partially attributed to posterior aortic support provided by the spine and right lateral support provided by the inferior vena cava. The findings may also suggest that the left lateral side of the aneurysm may be weaker and prone to enlargement [39]. Further work will be needed to determine if rupture on the left side of AAAs is a pattern that could potentially be used to improve risk stratification. Furthermore, our results suggest that above the knee amputations and iliac artery occlusion likely have different effects on infrarenal aorta hemodynamics, potentially due to the grade of stenosis and rate of collateral artery formation in the lower limbs. Collateral remodeling may compensate in some ways for iliac stenosis on aortic flow over extended periods. Conversely, and more consistent with our sudden onset model, above the knee amputation results in a rapid increase in vascular resistance [40, 41], which may exacerbate the disturbed triphasic flow pattern commonly observed in the infrarenal aorta [28, 41], possibly increasing the chances of asymmetric AAA formation. Validation in a larger human image dataset supported by further animal studies are needed for a true quantitative discrimination of the effects that iliac occlusion has on infrarenal aorta hemodynamics.

Conclusion

We show here that modified iliac outflow in mice leads to faster AAA growth and slightly larger aneurysms after 8 weeks, with variable time-dependent centerline shift and altered aneurysm morphology. Additionally, characteristic molecular patterns of AAA formation, such as TGFβ1 expression, were altered in animals with iliac stenosis. Human AAA patients showed leftward expansion of the aneurysm with highly variable centerline shift, regardless of iliac stenosis. Taking both mouse and human data into account, these results suggest that moderate iliac stenosis may have flow-dependent upstream effects on early AAA formation and progression due to a differential cellular activity in the aneurysm wall.

Supplementary Material

Refer to Web version on PubMed Central for supplementary material.

Acknowledgments

The authors would like to acknowledge Andrea Chambers for her ultrasound imaging assistance.

Funding Sources

Funding was provided to Dr. C.J.G. through the AHA Scientist Development Grant (14SDG18220010), G.S.S. and A.G.B through the NSF Graduate Research Fellowship (DGE-1333468), and G.S.S. through the NIH T32 Bioengineering Interdisciplinary Training for Diabetes Research (T32DK101001-05).

References

1. Sampson UK, Norman PE, Fowkes FG, Aboyans V, Song Y, Harrell FE Jr, et al. Estimation of global and regional incidence and prevalence of abdominal aortic aneurysms 1990 to 2010. Glob Heart. 2014 3;9(1):159–70. [PubMed: 25432125]
2. Sampson UKA, Norman PE, Fowkes FGR, Aboyans V, Song Y, Harrell FE Jr, et al. Global and regional burden of aortic dissection and aneurysms: mortality trends in 21 world regions, 1990 to 2010 Glob Heart. 2014 Mar; 9(1):171–80.e10.
3. Vardulaki KA, Prevost TC, Walker NM, Day NE, Wilmink AB, Quick CR, et al. Incidence among men of asymptomatic abdominal aortic aneurysms: estimates from 500 screen detected cases. J Med Screen. 1999;6(1):50–4. [PubMed: 10321373]
4. Wassef M, Baxter BT, Chisholm RL, Dalman RL, Fillinger MF, Heinecke J, et al. Pathogenesis of abdominal aortic aneurysms: a multidisciplinary research program supported by the National Heart, Lung, and Blood Institute. J Vasc Surg. 2001 10;34(4):730–8. [PubMed: 11668331]
5. Vollmar JF, Paes E, Pauschinger P, Henze E, Friesch A. Aortic aneurysms as late sequelae of above-knee amputation. Lancet. 1989 10; 2(8667):834–5. [PubMed: 2571760]
6. Lorenz M, Panitz K, Grosse-Furtner C, Meyer J, Lorenz R. Lower-limb amputation, prevalence of abdominal aortic aneurysm and atherosclerotic risk factors. Br J Surg. 1994 Jun; 81(6):839–40.
7. Vorp DA, Raghavan ML, Webster MW. Mechanical wall stress in abdominal aortic aneurysm: influence of diameter and asymmetry. J Vasc Surg. 1998 4;27(4):632–9. [PubMed: 9576075]
8. Fillinger MF, Racusin J, Baker RK, Cronenwett JL, Teutelink A, Schermerhorn ML, et al. Anatomic characteristics of ruptured abdominal aortic aneurysm on conventional CT scans: implications for rupture risk. J Vasc Surg. 2004 6;39(6):1243–52. [PubMed: 15192565]
9. Finol EA, Keyhani K, Amon CH. The effect of asymmetry in abdominal aortic aneurysms under physiologically realistic pulsatile flow conditions. J Biomech Eng. 2003 4;125(2): 207–17. [PubMed: 12751282]
10. Yeung JJ, Kim HJ, Abbruzzese TA, Vignon-Clementel IE, Draney-Blomme MT, Yeung KK, Perkash I, Herfkens RJ, Taylor CA, Dalman RL: Aortoiliac hemodynamic and morphologic

adaptation to chronic spinal cord injury. J Vasc Surg. 2006 12;44(6):1254–65. [PubMed: 17145427]

11. Rodriguez JF, Ruiz C, Doblare M, Holzapfel GA. Mechanical stresses in abdominal aortic aneurysms: influence of diameter, asymmetry, and material anisotropy. J Biomech Eng. 2008 4; 130(2):021023. [PubMed: 18412510]
12. Crawford JD, Chivukula VK, Haller S, Vatankhah N, Bohannan CJ, Moneta GL, et al. Aortic outflow occlusion predicts rupture of abdominal aortic aneurysm. J Vasc Surg. 2016 12;64(6): 1623–8. [PubMed: 27374068]
13. Hoshina K, Sho E, Sho M, Nakahashi TK, Dalman RL. Wall shear stress and strain modulate experimental aneurysm cellularity. J Vasc Surg. 2003 5;37(5):1067–74. [PubMed: 12756356]
14. Sho E, Sho M, Hoshina K, Kimura H, Nakahashi TK, Dalman RL. Hemodynamic forces regulate mural macrophage infiltration in experimental aortic aneurysms. Exp Mol Pathol. 2004 4;76(2): 108–16. [PubMed: 15010288]
15. Sho E, Sho M, Nanjo H, Kawamura K, Masuda H, Dalman RL. Hemodynamic regulation of CD34+ cell localization and differentiation in experimental aneurysms. Arterioscler Thromb Vasc Biol. 2004 10;24(10): 1916–21. [PubMed: 15319272]
16. Busch A, Chernogubova E, Jin H, Meurer F, Eckstein HH, Kim M, et al. Four Surgical Modifications to the Classic Elastase Perfusion Aneurysm Model Enable Haemodynamic Alterations and Extended Elastase Perfusion. Eur J Vasc Endovasc Surg. 2018 7; 56(1):102–9. [PubMed: 29703523]
17. Updegrove A, Wilson NM, Merkow J, Lan H, Marsden AL, Shadden SC. SimVascular: an open source pipeline for cardiovascular simulation. Ann Biomed Eng. 2017 3;45(3): 525–41. [PubMed: 27933407]
18. Schneider CA, Rasband WS, Eliceiri KW. NIH Image to ImageJ: 25 years of image analysis. Nat Methods. 2012 7;9(7):671–5. [PubMed: 22930834]
19. Abramoff MD, Magalhaes PJ, Ram SJ. Image processing with ImageJ. Biophoton Int. 2003; 11:36–42.
20. Busch A, Hartmann E, Grimm C, Ergun S, Kickuth R, Otto C, et al. Heterogeneous histomorphology, yet homogeneous vascular smooth muscle cell dedifferentiation, characterize human aneurysm disease. J Vasc Surg. 2017;66:1553–64.e1556. [PubMed: 27720318]
21. Berens P CircStat: a MATLAB toolbox for circular statistics. J Stat Softw. 2009;31(10): 1–21.
22. Dua MM, Dalman RL. Hemodynamic influences on abdominal aortic aneurysm disease: application of biomechanics to aneurysm pathophysiology. Vascul Pharmacol. 2010 Jul-Aug;53(1–2):11–21. [PubMed: 20347049]
23. Van Vickle-Chavez SJ, Tung WS, Absi TS, Ennis TL, Mao D, Cobb JP, et al. Temporal changes in mouse aortic wall gene expression during the development of elastase-induced abdominal aortic aneurysms. J Vasc Surg. 2006 5;43(5):1010–20. [PubMed: 16678698]
24. Juvonen J, Surcel HM, Satta J, Teppo AM, Bloigu A, Syrjala H, et al. Elevated circulating levels of inflammatory cytokines in patients with abdominal aortic aneurysm. Arterioscler Thromb Vasc Biol. 1997 11;17(11):2843–7. [PubMed: 9409264]
25. Choke E, Cockerill GW, Dawson J, Wilson RW, Jones A, Loftus IM, et al. Increased angiogenesis at the site of abdominal aortic aneurysm rupture. Ann N Y Acad Sci. 2006 11; 1085(1):315–9. [PubMed: 17182949]
26. Azuma J, Wong RJ, Morisawa T, Hsu M, Maegdefessel L, Zhao H, et al. Heme oxygenase-1 expression affects murine abdominal aortic aneurysm progression. PLoS One. 2016 2; 11(2):e0149288. [PubMed: 26894432]
27. Goergen CJ, Azuma J, Barr KN, Magdefessel L, Kallop DY, Gogineni A, et al. Influences of aortic motion and curvature on vessel expansion in murine experimental aneurysms. Arterioscler Thromb Vasc Biol. 2011 2;31(2): 270–9. [PubMed: 21071686]
28. Amirbekian S, Long RC Jr, Consolini MA, Suo J, Willett NJ, Fielden SW, et al. In vivo assessment of blood flow patterns in abdominal aorta of mice with MRI: implications for AAA localization. Am J Physiol Heart Circ Physiol. 2009 10;297(4):H1290–5. [PubMed: 19684182]

29. Correia M, Provost J, Tanter M, Pernot M. 4D ultrafast ultrasound flow imaging: in vivo quantification of arterial volumetric flow rate in a single heartbeat. Phys Med Biol. 2016 12;61(23):L48–61. [PubMed: 27811406]
30. Sangwung P, Zhou G, Nayak L, Chan ER, Kumar S, Kang DW, et al. KLF2 and KLF4 control endothelial identity and vascular integrity. JCI Insight. 2017 2;2(4):e91700. [PubMed: 28239661]
31. Westvik TS, Fitzgerald TN, Muto A, Maloney SP, Pimiento JM, Fancher TT, et al. Limb ischemia after iliac ligation in aged mice stimulates angiogenesis without arteriogenesis. J Vasc Surg. 2009 2;49(2):464–73. [PubMed: 19028053]
32. Lareyre F, Clement M, Raffort J, Pohlod S, Patel M, Esposito B, et al. TGFp (Transforming Growth Factor-β) Blockade Induces a Human-Like Disease in a Nondissecting Mouse Model of Abdominal Aortic Aneurysm. Arterioscler Thromb Vasc Biol. 2017 11;37(11): 2171–81. [PubMed: 28912363]
33. Gao F, Chambon P, Offermanns S, Tellides G, Kong W, Zhang X, et al. Disruption of TGF-β signaling in smooth muscle cell prevents elastase-induced abdominal aortic aneurysm. Biochem Biophys Res Commun. 2014 11; 454(1):137–43. [PubMed: 25450370]
34. Dietz HC. TGF-β in the pathogenesis and prevention of disease: a matter of aneurysmic proportions. J Clin Invest. 2010 2; 120(2): 403–7. [PubMed: 20101091]
35. Pyo R, Lee JK, Shipley JM, Curci JA, Mao D, Ziporin SJ, et al. Targeted gene disruption of matrix metalloproteinase-9 (gelatinase B) suppresses development of experimental ab-dominal aortic aneurysms. J Clin Invest. 2000 6;105(11): 1641–9. [PubMed: 10841523]
36. Bhamidipati CM, Mehta GS, Lu G, Moehle CW, Barbery C, DiMusto PD, et al. Development of a novel murine model of aortic aneurysms using peri-adventitial elastase. Surgery. 2012 8;152(2): 238–46. [PubMed: 22828146]
37. Lu G, Su G, Davis JP, Schaheen B, Downs E, Roy RJ, et al. A novel chronic advanced stage abdominal aortic aneurysm murine model. J Vasc Surg. 2017 7;66(1):232–242.e4. [PubMed: 28274752]
38. Busch A, Holm A, Wagner N, Ergun S, Rosenfeld M, Otto C, et al. Extra-and intraluminal elastase induce morphologically distinct abdominal aortic aneurysms in mice and thus represent specific subtypes of human disease. J Vasc Res. 2016;53(1–2):49–57. [PubMed: 27532120]
39. Assar AN, Zarins CK. Ruptured abdominal aortic aneurysm: a surgical emergency with many clinical presentations. Postgrad Med J. 2009 5;85(1003):268–73. [PubMed: 19520879]
40. Paula-Ribeiro M, Garcia MM, Martinez DG, Lima JR, Laterza MC. Increased peripheral vascular resistance in male patients with traumatic lower limb amputation: one piece of the cardiovascular risk puzzle. Blood Press Monit. 2015 12;20(6):341–5. [PubMed: 26274369]
41. Padilla J, Jenkins NT, Laughlin MH, Fadel PJ. Blood pressure regulation VIII: resistance vessel tone and implications for a proatherogenic conduit artery endothelial cell phenotype. Eur J Appl Physiol. 2014 3;114(3): 531–44. [PubMed: 23860841]

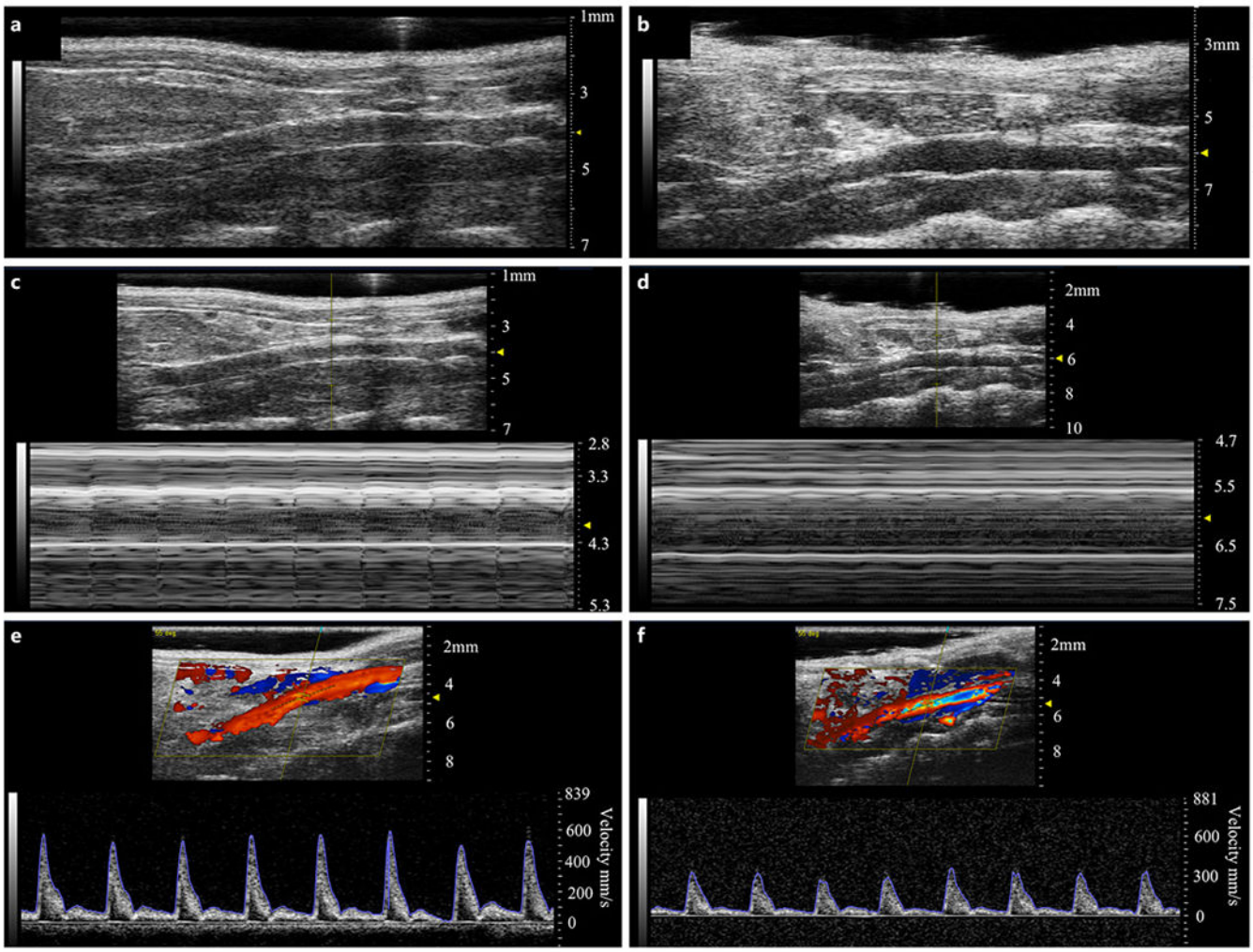

Fig. 1.

Representative healthy (left panels) and aneurysmal (right panels) murine aortae with B-mode (**a**, **b**), M-mode (**c**, **d**), and PWD (**e**, **f**) images. B-mode images were used to assess overall vessel structure and quantify the increase in aortic diameter after PPE treatment. M-mode was used to measure circumferential cyclic strain, and PWD was used to quantify mean and peak velocities.

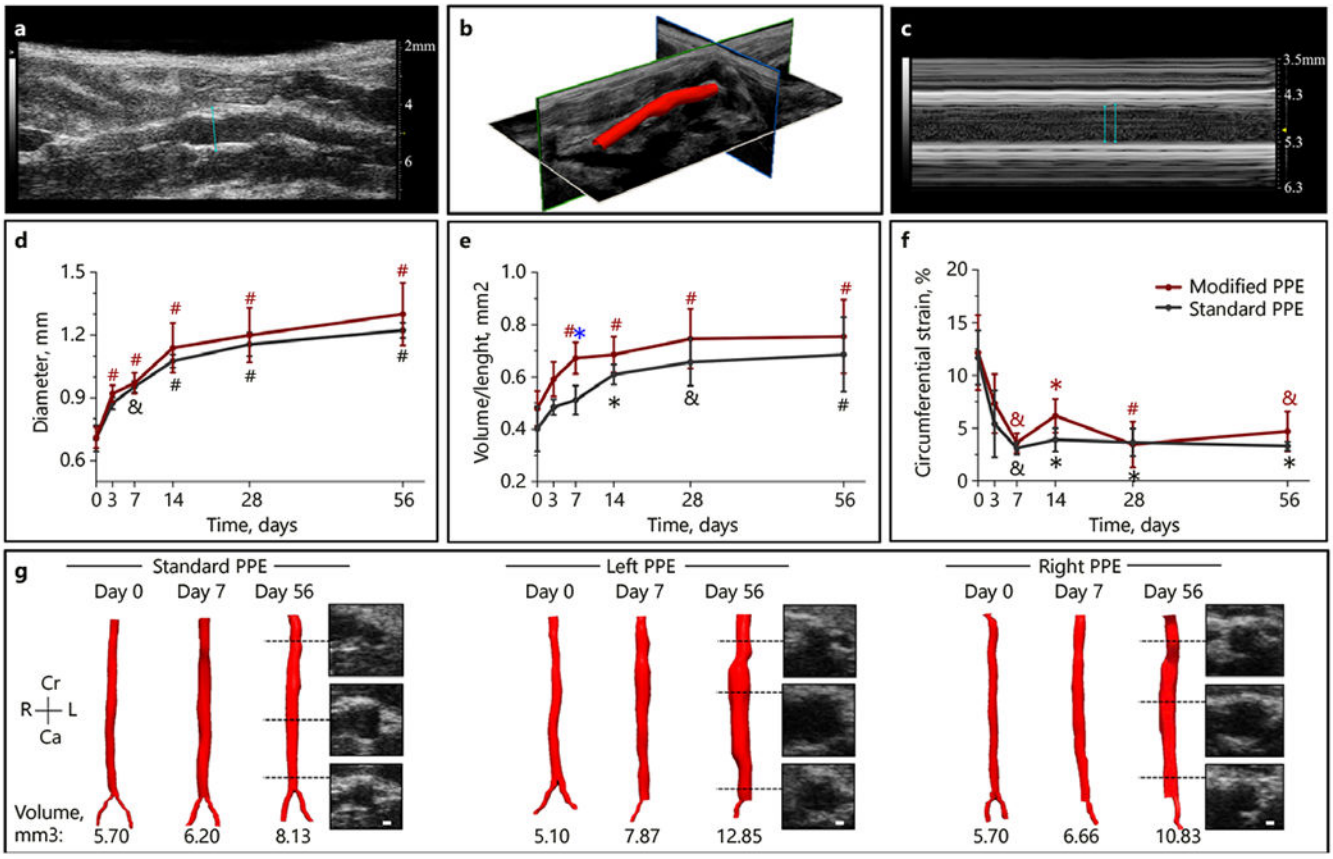

Fig. 2.

Summary of structural changes in murine abdominal aortic aneurysm development among standard, left, and right PPE groups. Long-axis B-mode was used to quantify aortic diameter (**a**), 3D ultrasound for aortic segmentation and volume characterization (**b**), and M-mode to quantify systolic and diastolic diameters (**c**) that were used to assess changes in circumferential cyclic strain. The aortic diameter continues to increase up to day 56 (**d**) with the modified PPE group having a rapid increase in volume/length up to day 7 (**e**). We also observed a sharp decrease in circumferential cyclic strain between baseline and day 7 post-procedure time points (**f**). Representative short-axis ultrasound, 3D segmentation, and volume showed slightly larger aneurysm in the modified PPE group compared to the standard PPE group (**g**). Statistical significance compared with day 0 and defined at * $p < 0.05$, $^{\&}$ $p < 0.01$, and $^{\#}$ $p < 0.001$. The blue asterisk (**e**) represents statistical significance between the standard and modified PPE groups.

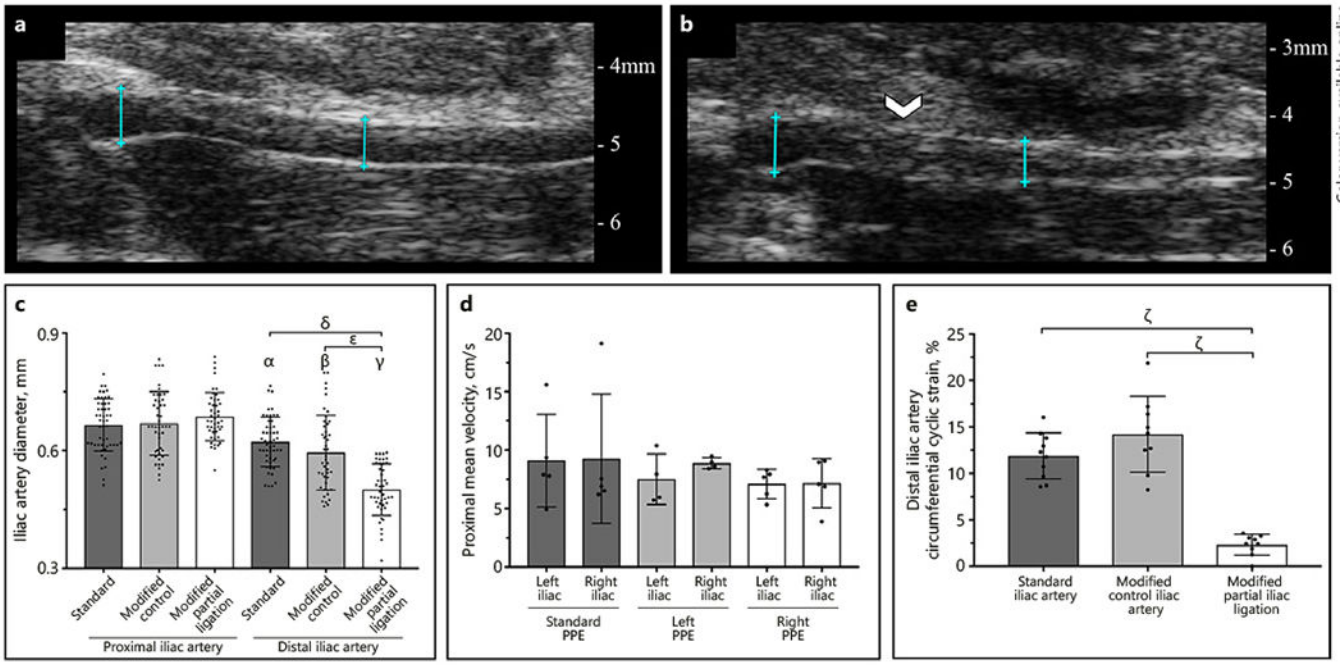

Fig. 3.

Comparison of structural and hemodynamic changes between non-ligated (**a**) and partially ligated (**b**) iliac arteries at day 56. We observed a significant decrease in diameter (**c**) and circumferential cyclic strain (**e**) in modified iliac arteries compared to standard PPE arteries and contralateral control iliac arteries. We did not, however, see significant changes in iliac artery velocity between standard and modified PPE groups at day 56 (**d**). Suture placement is highlighted by the white arrow and diameter measurement locations are shown by blue lines. Statistical significance is shown as $p < 0.001$ (α, β, γ, δ, ε, ζ). Symbols α, β, γ signify statistical significance between their respective group and the standard, modified control, and modified partial ligation groups in the proximal iliac artery.

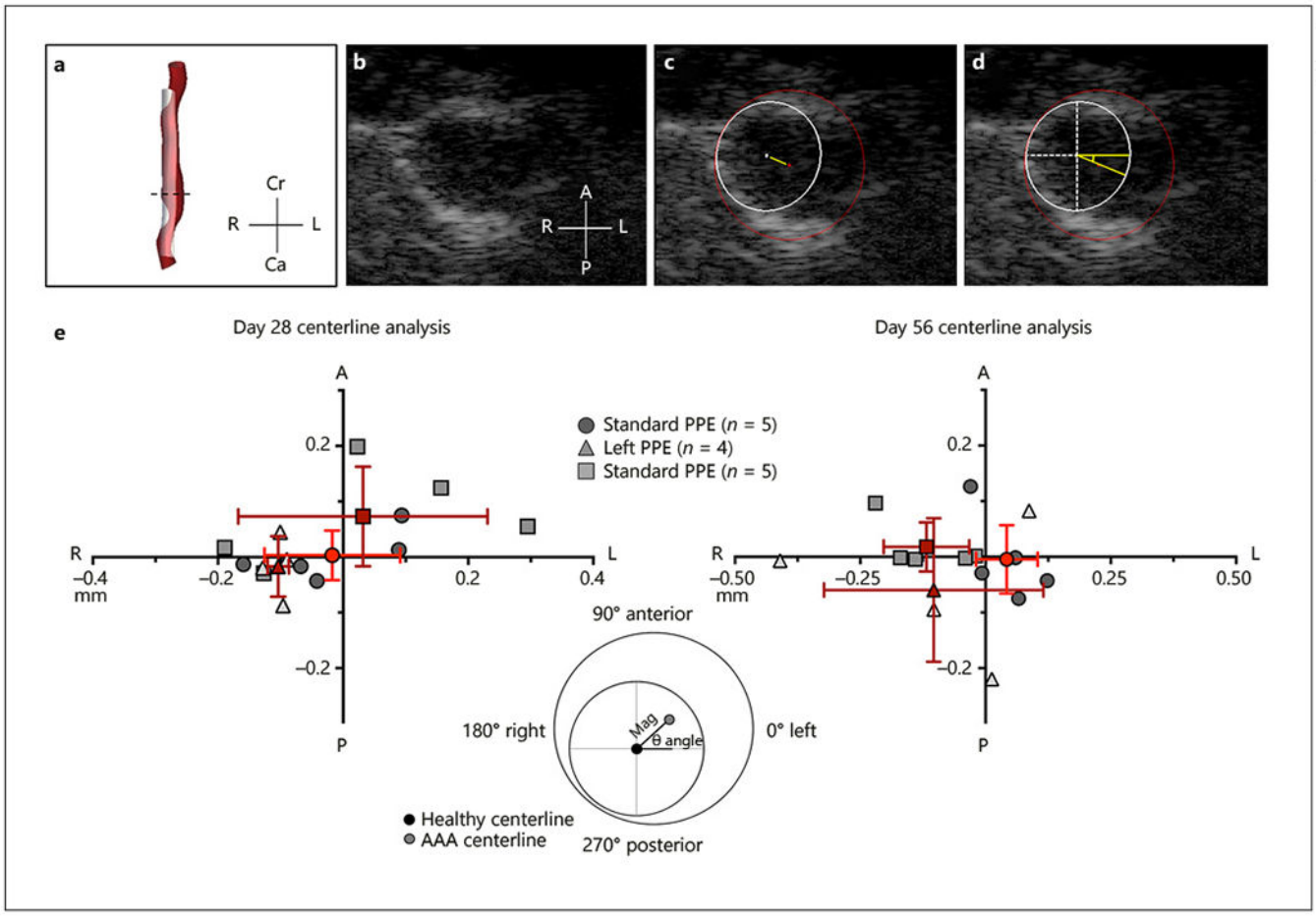

Fig. 4.

Summary of murine centerline deviation analysis methods and results. Aneurysm and projected healthy regions were first segmented using SimVascular (**a**). We then used short-axis view (**b**) to quantify magnitude (**c**) and direction (**d**) of centerline deviation between the healthy and diseased aorta. Centerline deviation results (**e**) for day 28 and 56 shows the shift in magnitude and direction of the diseased vessels with respect to the healthy vessel. Red points represent the mean centerline deviation for the standard and modified PPE groups, and the red lines represent the standard deviation in the *x* and *y* axes. Cr, cranial; Ca, caudal; L, left; R, right; A, anterior; P, posterior.

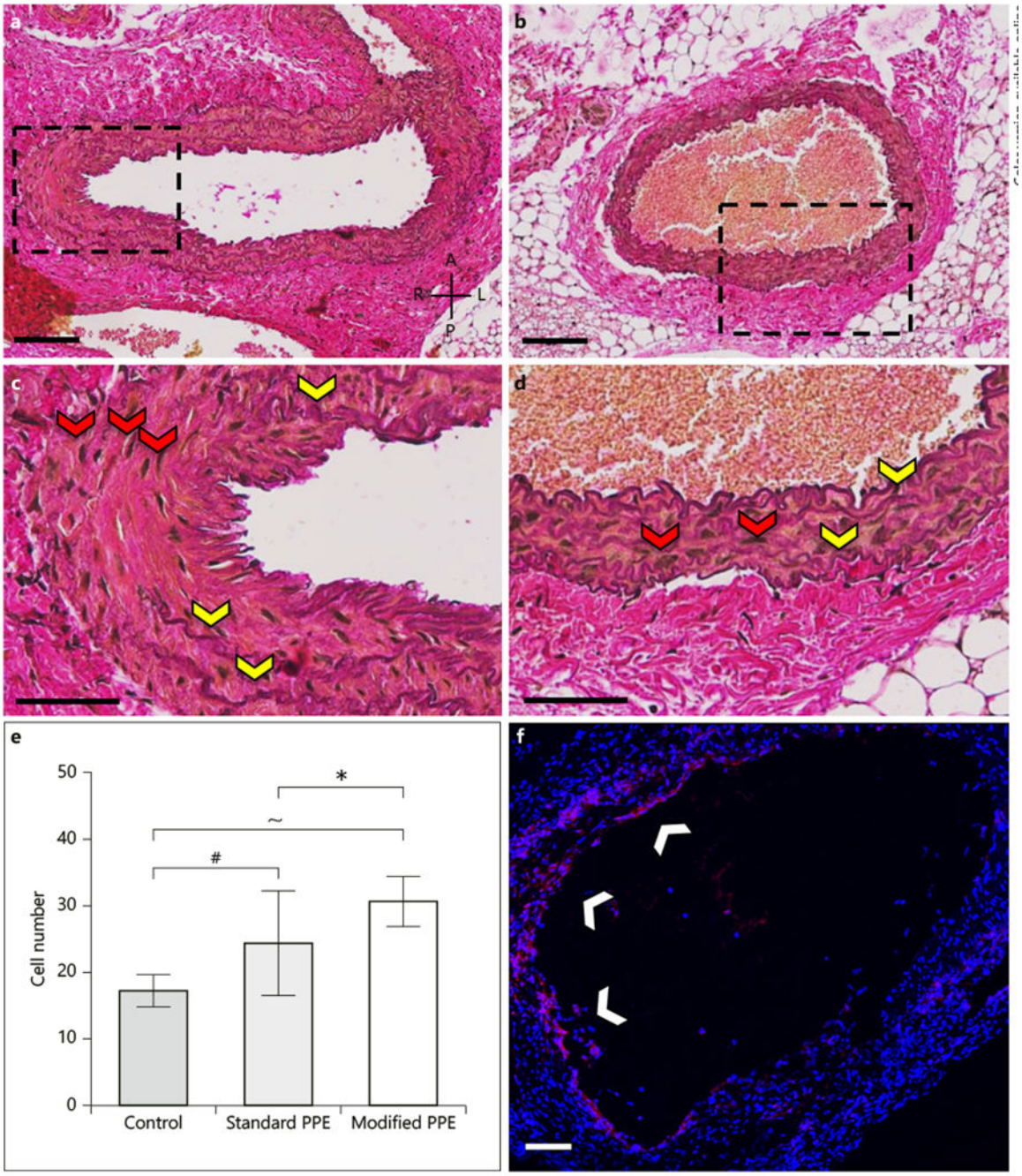

Fig. 5.

Histological and immunohistochemistry analysis of PPE-infused aortic tissue consisting of EvG-stained standard (**a, c**) and modified (**b, d**) aortae, as well as Ki67-stained modified (**f**) infrarenal aorta. Histology shows diffuse elastin breakage throughout the vessels (yellow arrows), thus confirming aneurysm induction. Ki67 staining shows cell proliferation in the standard and modified PPE animals (white arrows). Further, cell number analysis showed a significant increase in cell nuclei (red arrows) between the modified and standard PPE-

infused aortae (**h**). A, anterior; P, posterior; L, left; R, right. Scale bars = 100 μm (**a, c**) and 50 μm (**b, d**). Statistical significance is defined at * $p < 0.05$, # $p < 0.001$, ~ $p < 0.0001$.

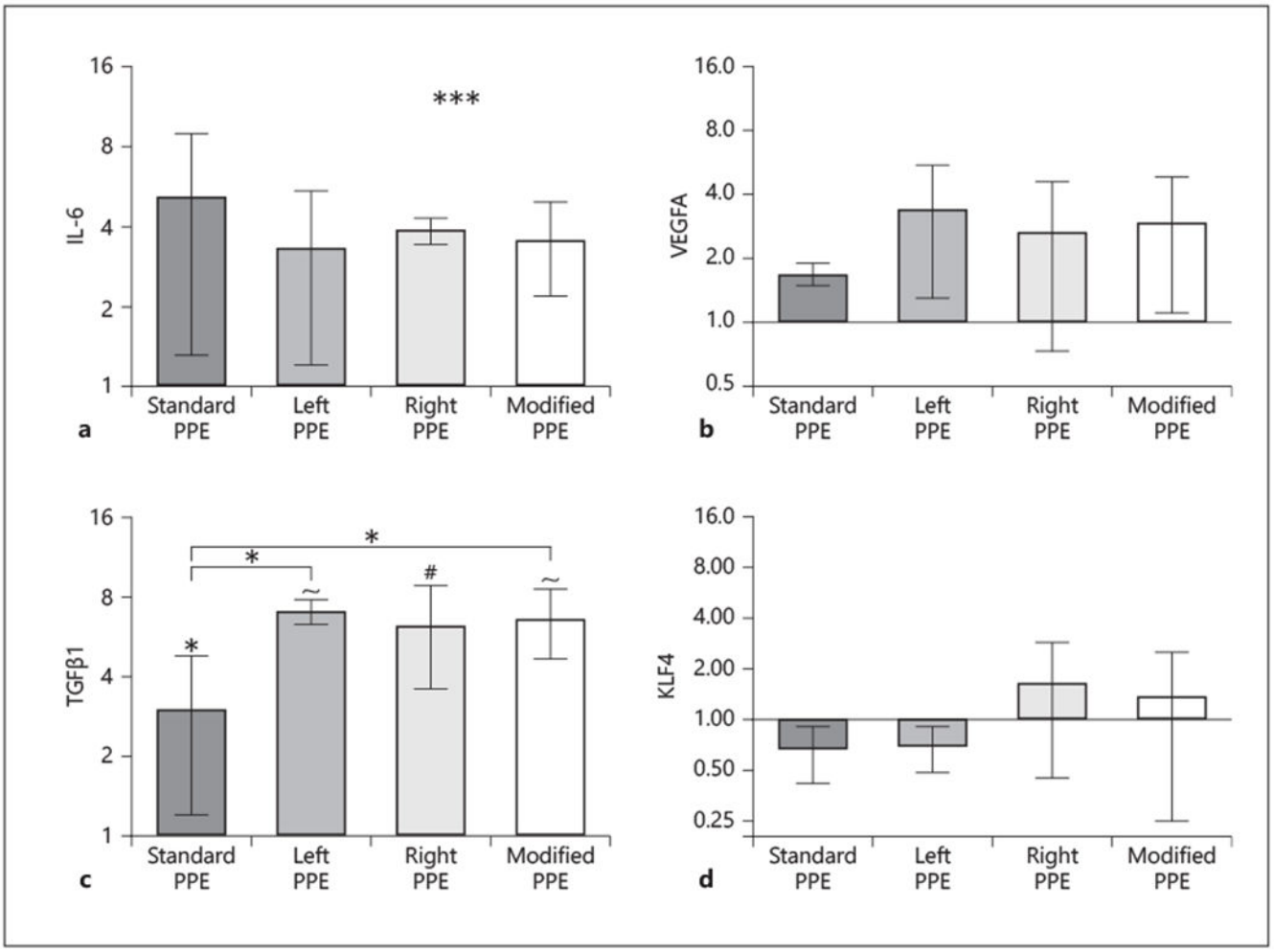

Fig. 6.

Relative gene expression analysis of standard and modified infrarenal aortae at day 56 using qPCR. IL-6 (**a**) and VEGFA (**b**) are upregulated, but there are no significant differences between PPE-infused and control aortae. TGFβ1 shows significant upregulation between PPE-infused and control aortae, and standard and modified groups (**c**); while KLF4 (**d**) shows variable differences in expression between standard and modified groups. Fold change values are relative to control aortae. Statistical significance is defined at * $p < 0.05$, # $p < 0.001$, and ~ $p < 0.0001$.

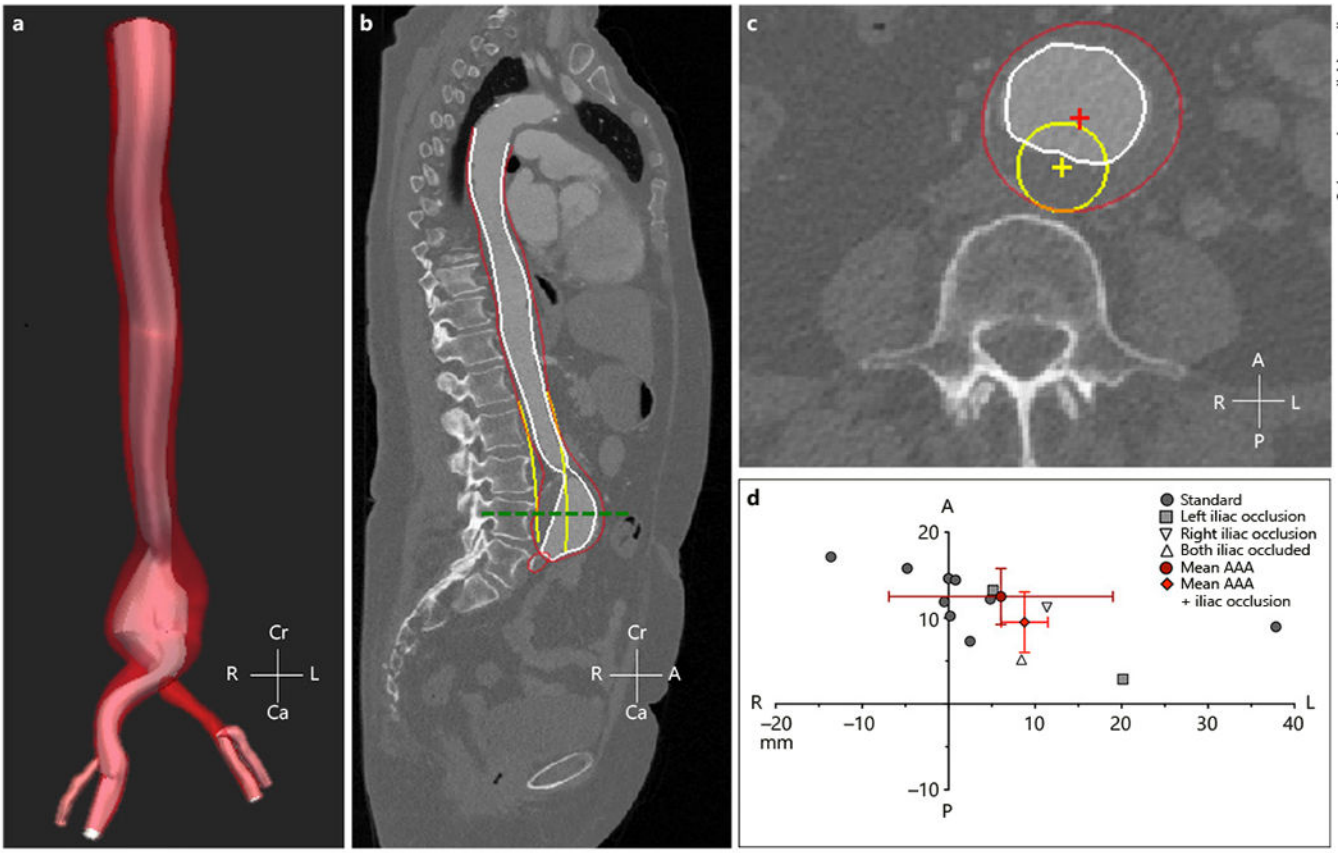

Fig. 7.

Summary of human centerline deviation analysis methods and results. 3D segmentation was performed on human AAA (**a**) and a sagittal cross-sectional plane was used to confirm quality of 3D segmentation with red, white, and yellow highlighting the AAA wall, AAA lumen, and projected healthy aorta, respectively (**b**). A transverse cross-sectional plane along the center of the AAA (green dashed line) was used to quantify magnitude and direction of centerline deviation (**c**). Quantitative analysis shows that standard and modified AAA grew away from the spine in the leftward direction, likely due to the natural leftward origin of the healthy aorta. Red points represent the mean centerline deviation for the standard and modified PPE groups, and the red lines represent the standard deviation in the *x* and *y* axes. Cr, cranial; Ca, caudal; L, left; R, right; A, anterior; P, posterior.